NON-NEGATIVE TENSOR FACTORIZATION USING ALPHA AND BETA DIVERGENCES

Andrzej CICHOCKI[1*], *Rafal ZDUNEK*[1†], *Seungjin CHOI*[2], *Robert PLEMMONS*[3], *Shun-ichi AMARI*[1]

[1] Brain Science Institute, RIKEN, Wako-shi, Saitama 351-0198, JAPAN,
[2] Pohang University of Science and Technology, KOREA,
[3] Wake Forest University, USA

ABSTRACT

In this paper we propose new algorithms for 3D tensor decomposition/factorization with many potential applications, especially in multi-way Blind Source Separation (BSS), multidimensional data analysis, and sparse signal/image representations. We derive and compare three classes of algorithms: Multiplicative, Fixed-Point Alternating Least Squares (FPALS) and Alternating Interior-Point Gradient (AIPG) algorithms. Some of the proposed algorithms are characterized by improved robustness, efficiency and convergence rates and can be applied for various distributions of data and additive noise.

Index Terms— Optimization, Learning systems, Linear approximation, Signal representations, Feature extraction.

1. MODELS AND PROBLEM FORMULATION

Tensors (also known as n-way arrays or multidimensional arrays) are used in a variety of applications ranging from neuroscience and psychometrics to chemometrics [1, 2, 3, 4]. Non-negative Matrix Factorization (NMF), Non-negative Tensor Factorization (NTF) and parallel factor analysis PARAFAC models with non-negativity constraints have been recently proposed as sparse and quite efficient representations of signals, images, or general data [2, 3, 4, 5, 6, 7, 8, 9, 10, 11]. From a viewpoint of data analysis, NTF is very attractive because it takes into account spacial and temporal correlations between variables more accurately than 2D matrix factorizations, such as NMF, and it usually provides sparse common factors or hidden (latent) components with physiological meaning and interpretation [4]. In most applications, especially in neuroscience (EEG, fMRI), the standard NTF or PARAFAC models were used [8, 12, 13]. In this paper we consider more general model referred to as a 3D NTF2 model (in analogy to the Parafac2 model [4]) (see Fig. 1). A given tensor $\underline{X} \in \mathbb{R}_+^{I \times T \times K}$ is decomposed into a set of matrices S, D and $\{A_1, A_2, ..., A_K\}$ with non-negative entries. Here and elsewhere, $\mathbb{R}_+$ denotes the non-negative orthant with appropriate

---
[*]On leave from Warsaw University of Technology, POLAND
[†]On the leave from Institute of Telecommunications, Teleinformatics, and Acoustics, Wroclaw University of Technology, POLAND

dimensions. The three-way NTF2 model can be described as

$$X_k = A_k D_k S + E_k, \qquad (k = 1, 2, \ldots, K) \qquad (1)$$

where $X_k = X_{:,:,k} = [x_{itk}]_{I \times T} \in \mathbb{R}_+^{I \times T}$ are frontal slices of $\underline{X} \in \mathbb{R}_+^{I \times T \times K}$, K is the number of frontal slices, $A_k = [a_{irk}]_{I \times R} \in \mathbb{R}_+^{I \times R}$ are the basis (mixing matrices), $D_k \in \mathbb{R}_+^{R \times R}$ is a diagonal matrix that holds the k-th row of the $D \in \mathbb{R}_+^{K \times R}$ in its main diagonal, and $S = [s_{rt}]_{R \times T} \in \mathbb{R}_+^{R \times T}$ is a matrix representing sources (or hidden components or common factors), and $E_k = E_{:,:,k} \in \mathbb{R}^{I \times T}$ is the k-th frontal slice of a tensor $\underline{E} \in \mathbb{R}^{I \times T \times K}$ representing error or noise depending upon the application. The objective is to estimate the set of matrices $\{A_k\}, (1, \ldots, k, \ldots, K)$, D and S, subject to some non-negativity constraints and other possible natural constraints such as sparseness and/or smoothness. Since the diagonal matrices D_k are scaling matrices they can usually be absorbed by the matrices A_k by introducing column-normalized matrices $A_k := A_k D_k$, so usually in BSS applications the matrix S and the set of scaled matrices $A_1, \ldots, A_K$ need only to be estimated. However, in such a case we may loose the uniqueness of the NTF representation ignoring scaling and permutation ambiguities. The uniqueness still can be achieved by imposing nonnegativity, sparsity and other constraints. The above NTF2 model is similar to the well known PARAFAC2 model with non-negativity constraints and Tucker models [2, 12, 4]. In the special case, when all matrices A_k are identical, the NTF2 model can be simplified to the ordinary PARAFAC model with the non-negativity constraints described as $X_k = A D_k S + E_k$, $k = 1, \ldots, K$ or equivalently $x_{itk} = \sum_r a_{ir} s_{rt} d_{kr} + e_{itk}$ or $\underline{X} = \sum_r a_r \otimes s_r^T \otimes d_r + \underline{E}$, where s_r are rows of S and a_r, d_r are columns of A and D, respectively, and $\otimes$ means outer product of vectors [3]. Throughout this paper, we use the following notation: the rt-th element of the matrix S is denoted by s_{rt}, $x_{itk} = [X_k]_{it}$ means the it-th element of the k-th frontal slice X_k, $\bar{A} = [A_1; A_2; \ldots; A_K] \in \mathbb{R}_+^{KI \times R}$ is a column-wise unfolded matrix of the slices A_k, $\bar{a}_{pr} = [\bar{A}]_{pr}$. Similarly, $\bar{X} = [X_1; X_2; \ldots; X_K] \in \mathbb{R}_+^{KI \times T}$ is the column-wise unfolded matrix of the slices X_k, $\bar{x}_{pt} = [\bar{X}]_{pt}$.
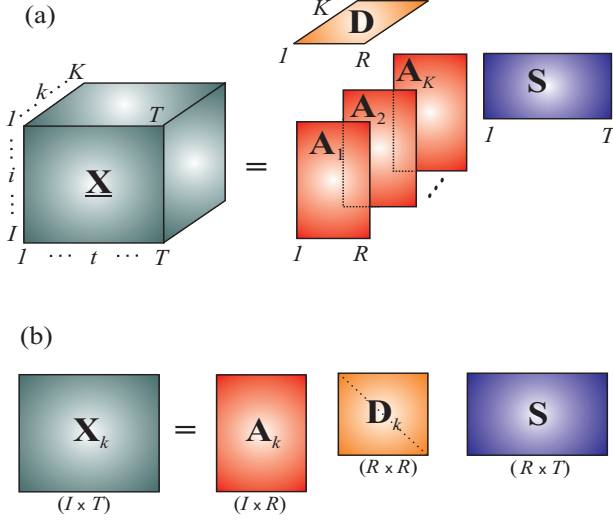
Fig. 1. (a) NTF2 model in which a 3D tensor is decomposed into a set of non-negative matrices: $\{A_1, \ldots, A_K\}$, D, S. (b) Equivalent representation in which frontal slices of a tensor are factored by a set of matrices (tensor $\underline{E}$ representing error is omitted for simplicity).

2. ALPHA AND BETA DIVERGENCES

To deal with the model (1) efficiently we adopt several approaches from constrained multi-criteria optimization, where we minimize simultaneously several cost functions using alternating switching between sets of parameters. The α and β-divergences are two complimentary generalized cost functions which can be applied for NMF and NTF [1, 6, 7, 8].

2.1. α-divergence

Let us consider a flexible and general class of the cost functions, called α-divergence [1, 6]:

$$D_A^{(\alpha)}(\bar{X}||\bar{A}S) = \frac{\sum_{pt}(\bar{x}_{pt}^\alpha[\bar{A}S]_{pt}^{1-\alpha} - \alpha\bar{x}_{pt} + (\alpha-1)[\bar{A}S]_{pt})}{\alpha(\alpha-1)}$$

$$D_{Ak}^{(\alpha)}(X_k||A_kS) = \sum_{it} \frac{x_{itk}^\alpha[A_kS]_{it}^{1-\alpha}}{\alpha(\alpha-1)} - \frac{x_{itk}}{\alpha-1} + \frac{[A_kS]_{it}}{\alpha}$$

We note that as special cases of α-divergence for $\alpha = 2, 0.5, -1$, we obtain the Pearson's, Hellinger's and Neyman's chi-square distances [6], respectively. Evaluating the limits for $\alpha \to 1$ and $\alpha \to 0$, one obtains the generalized Kullback-Leibler (KL) divergence (I-divergence) and the dual generalized KL divergence, respectively [6, 7, 8].

Instead of applying the standard gradient descent method, we use the nonlinearly transformed gradient approach as gen-

eralization of the exponentiated gradient (EG) [7]:

$$\Phi(a_{irk}) \leftarrow \Phi(a_{irk}) - \eta_{irk} \frac{\partial D_{A_k}^{(\alpha)}(X_k||A_kS)}{\partial \Phi(a_{irk})}, \quad (2)$$

$$\Phi(s_{rt}) \leftarrow \Phi(s_{rt}) - \eta_{rt} \frac{\partial D_A^{(\alpha)}(\bar{X}||\bar{A}S)}{\partial \Phi(s_{rt})}, \quad (3)$$

where $\Phi(x)$ is a suitably chosen function.

It can be shown that such a nonlinear transformation provides a stable solution and the gradients are much better behaved in the space Φ. In our case, we employ $\Phi(x) = x^\alpha$, which leads directly to the new learning algorithm (for $\alpha \neq 0$) (the rigorous proof of local convergence similar to this given by Lee and Seung [11] is omitted due to a lack of space):

$$a_{irk} \leftarrow a_{irk} \left(\frac{\sum_{t=1}^T (x_{itk}/[A_kS]_{it})^\alpha s_{rt}}{\sum_{t=1}^T s_{rt}} \right)^{1/\alpha}, \quad (4)$$

$$s_{rt} \leftarrow s_{rt} \left(\frac{\sum_{p=1}^{KI} \bar{a}_{pr} (\bar{x}_{pt}/[\bar{A}S]_{pt})^\alpha}{\sum_{p=1}^{KI} \bar{a}_{pr}} \right)^{1/\alpha}. \quad (5)$$

2.2. β-divergence

Regularized β-divergence [14] for the NTF2 problem can be defined as follows:

$$D^{(\beta)}(\bar{X}||\bar{A}S) = \sum_{pt} (\bar{x}_{pt} \frac{\bar{x}_{pt}^\beta - [\bar{A}S]_{pt}^\beta}{\beta(\beta+1)}$$

$$+ [\bar{A}S]_{pt}^\beta \frac{[\bar{A}S]_{pt} - \bar{x}_{pt}}{\beta+1}) + \alpha_S\|S\|_{L1}, \quad (6)$$

$$D_k^{(\beta)}(X_k||A_kS) = \sum_{it} (x_{itk} \frac{x_{itk}^\beta - [A_kS]_{it}^\beta}{\beta(\beta+1)}$$

$$+ [A_kS]_{it}^\beta \frac{[A_kS]_{it} - x_{itk}}{\beta+1}) + \alpha_{A_k}\|A_k\|_{L1}, \quad (7)$$

$$k = 1, \ldots, K, \quad t = 1, 2, \ldots, T, \quad i = 1, 2, \ldots, I,$$

where α_S and α_{A_k} are small positive regularization parameters which control the degree of sparseness of the matrices S and A_k, respectively, and the $L1$-norms defined as $\|S\|_{L1} = \sum_{rt}|s_{rt}|$ and $\|A_k\|_{L1} = \sum_{ir}|a_{irk}|$ are introduced to enforce sparse representations of the solutions. It is interesting to note that for $\beta = 1$, we obtain the squared Euclidean distances expressed by the Frobenius norms $\|X_k - A_kS\|_F^2$, while for the singular cases, $\beta = 0$ and $\beta = -1$, the β-divergence has to be defined as limiting cases as $\beta \to 0$ and $\beta \to -1$, respectively. When these limits are evaluated one gets for $\beta \to 0$ the generalized KL divergence, and for $\beta \to -1$ we obtain the Itakura-Saito distance. The choice of the parameter β depends on the statistical distribution of the data and the β-divergence corresponds to the Tweedie models [14]. For example, the optimal choice of the parameter for the normal distribution is $\beta = 1$, for the γ-distribution

is $\beta \rightarrow -1$, for the Poisson distribution $\beta \rightarrow 0$, and for the compound Poisson $\beta \in (-1, 0)$. By minimizing the β-divergence, we have derived various kinds of NTF algorithms: Multiplicative based on the standard gradient descent, Exponentiated Gradient (EG), Projected Gradient (PG), Alternating Interior-Point Gradient (AIPG), or Fixed Point Alternating Least Squares (FPALS) algorithms. For example, in order to derive a flexible multiplicative learning algorithm, we compute the gradient of (6)-(7) with respect to elements of matrices $s_{rt} = s_r(t) = [\boldsymbol{S}]_{rt}$ and $a_{irk} = [\boldsymbol{A}_k]_{ir}$ and performing simple mathematical manipulations we obtain the multiplicative update rules:

$$a_{irk} \leftarrow a_{irk} \frac{[\sum_{t=1}^{T}(x_{itk}/[\boldsymbol{A}_k\boldsymbol{S}]_{it}^{1-\beta})\, s_{rt} - \alpha_{A_k}]_\varepsilon}{\sum_{t=1}^{T}[\boldsymbol{A}_k\boldsymbol{S}]_{it}^{\beta}\, s_{rt}}, \quad (8)$$

$$s_{rt} \leftarrow s_{rt} \frac{[\sum_{p=1}^{KI}\bar{a}_{pr}\,(\bar{x}_{itk}/[\bar{\boldsymbol{A}}\boldsymbol{S}]_{it}^{1-\beta}) - \alpha_S]_\varepsilon}{\sum_{p=1}^{KI}\bar{a}_{pr}\,[\bar{\boldsymbol{A}}_k\boldsymbol{S}]_{it}^{\beta}}, \quad (9)$$

where $[x]_\varepsilon = \max\{\varepsilon, x\}$ with a small $\varepsilon = 10^{-16}$ is introduced in order to avoid zero and negative values.

In the special case for $\beta = 1$ we have derived a new alternative algorithm, called regularized FPALS (Fixed Point Alternating Least Squares) algorithm (see [8] for details)

$$\boldsymbol{A}_k \leftarrow \left[(\boldsymbol{X}_k\boldsymbol{S}^T - \alpha_{A_k}\boldsymbol{E}_A)(\boldsymbol{S}\boldsymbol{S}^T + \gamma_S\boldsymbol{E})^+\right]_\varepsilon, \quad (10)$$

$$\boldsymbol{S} \leftarrow \left[(\bar{\boldsymbol{A}}^T\bar{\boldsymbol{A}} + \gamma_A\boldsymbol{E})^+(\bar{\boldsymbol{A}}^T\bar{\boldsymbol{X}} - \alpha_S\boldsymbol{E}_S)\right]_\varepsilon, \quad (11)$$

where γ_A, γ_S are small nonnegative regularization coefficients (typically, decaying to zero during iteration process), $\boldsymbol{A}^+$ denotes Moore-Penrose pseudo-inverse of $\boldsymbol{A}$ and $\boldsymbol{E}_A \in \mathbb{R}^{I \times R}$, $\boldsymbol{E}_S \in \mathbb{R}^{R \times T}$, $\boldsymbol{E} \in \mathbb{R}^{R \times R}$ are matrices with all entries one.

Furthermore, using the Alternating Interior-Point Gradient (AIPG) approach [15], another efficient algorithm has been developed and implemented [8]:

$$\boldsymbol{A}_k \leftarrow \boldsymbol{A}_k - \eta_{A_k}\boldsymbol{P}_{A_k}, \quad (12)$$

$$\boldsymbol{S} \leftarrow \boldsymbol{S} - \eta_S\boldsymbol{P}_S, \quad (13)$$

where $\boldsymbol{P}_{A_k} = \left(\boldsymbol{A}_k \oslash (\boldsymbol{A}_k\boldsymbol{S}\boldsymbol{S}^T)\right) \odot \left((\boldsymbol{A}_k\boldsymbol{S} - \boldsymbol{X}_k)\boldsymbol{S}^T\right)$, $\boldsymbol{P}_S = \left(\boldsymbol{S} \oslash (\bar{\boldsymbol{A}}^T\bar{\boldsymbol{A}}\boldsymbol{S})\right) \odot \left(\bar{\boldsymbol{A}}^T(\bar{\boldsymbol{A}}\boldsymbol{S} - \bar{\boldsymbol{X}})\right)$ and signs $\odot$ and $\oslash$ mean component-wise multiplication and division, respectively. The learning rates η_{A_k} and η_S are selected in this way to ensure the steepest descent, and on the other hand, to maintain non-negativity. Thus, $\eta_S = \min\{\tau\hat{\eta}_S, \eta_S^*\}$ and $\eta_{A_k} = \min\{\tau\hat{\eta}_{A_k}, \eta_{A_k}^*\}$, where $\tau \in (0, 1)$, $\hat{\eta}_S = \{\eta : \boldsymbol{S} - \eta\boldsymbol{P}_S\}$ and $\hat{\eta}_{A_k} = \{\eta : \boldsymbol{A}_k - \eta\boldsymbol{P}_{A_k}\}$ ensure non-negativity, and

$$\eta_{A_k}^* = \frac{\text{vec}(\boldsymbol{P}_{A_k})^T\text{vec}(\boldsymbol{A}_k\boldsymbol{S}\boldsymbol{S}^T - \boldsymbol{X}_k\boldsymbol{S}^T)}{\text{vec}(\boldsymbol{P}_{A_k}\boldsymbol{S})^T\text{vec}(\boldsymbol{P}_{A_k}\boldsymbol{S})}, \quad (14)$$

$$\eta_S^* = \frac{\text{vec}(\boldsymbol{P}_S)^T\text{vec}(\bar{\boldsymbol{A}}^T\bar{\boldsymbol{A}}\boldsymbol{S} - \bar{\boldsymbol{A}}^T\bar{\boldsymbol{X}})}{\text{vec}(\boldsymbol{A}_k\boldsymbol{P}_S)^T\text{vec}(\boldsymbol{A}_k\boldsymbol{P}_S)} \quad (15)$$

are the adaptive steepest descent learning rates.

3. SIMULATION RESULTS

All the NMF algorithms discussed in this paper have been extensively tested for many difficult benchmarks for signals and images with various statistical distributions and also for real EEG data. We found the best performance can be obtained with the AIPG, FPALS and the algorithm (8)-(9) for $\beta = 1$.

Due to space limitation, we present here only one simulation example. Nine natural highly correlated images are mixed by a randomly generated 3D tensor $\underline{\boldsymbol{A}} \in \mathbb{R}_+^{18 \times 9 \times 10}$. The observed mixed data are collected in 3D tensor $\underline{\boldsymbol{X}} \in \mathbb{R}_+^{18 \times 256^2 \times 10}$. The exemplary results are shown in Fig.2.

(a)   (b)
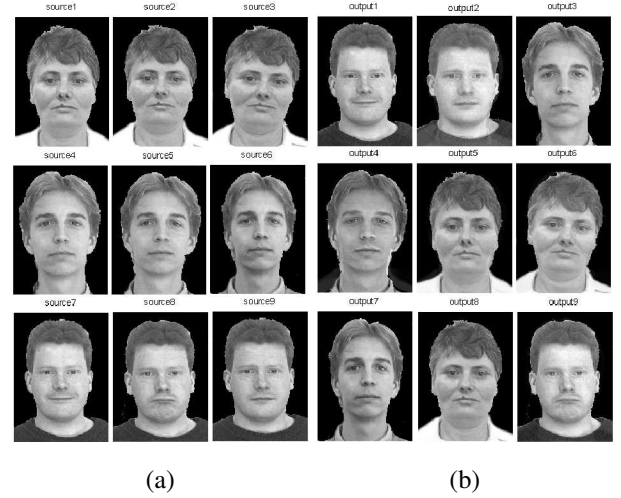
Fig. 2. Example: (a) 9 original source images; (b) estimated source images using FPALS algorithm (SIR = 32.9, 10.1, 45, 18.8, 28.2, 24.5, 42.2, 37.8, 27.1 [dB], respectively).

Table 1. Mean SIRs in [dB] obtained from 100 MC samples for estimation of the columns in the tensor $\underline{\boldsymbol{A}} \in \mathbb{R}^{I \times R \times K}$ and the rows (sources) in $\boldsymbol{S} \in \mathbb{R}^{R \times T}$ for the selected algorithms. The right column presents the elapsed times [in seconds] for a simple MC sample. In the experiments, the spectra signals are used.

ALGORITHMS:	$\underline{\boldsymbol{A}}$	$\boldsymbol{S}$	Times [s]
Alpha Alg. (4) – (5): $\alpha = 0.5$	21	17.9	31.7
Beta Alg. (8) – (9): $\beta = 1$	20.8	17.8	7.6
AIPG (12) – (15)	27.2	25	4.7
FPALS (10) – (11)	24.5	23.3	1.8

4. CONCLUSIONS AND DISCUSSION

In this paper we proposed generalized and flexible cost functions (controlled by a single parameter α or β) that allows us to derive a family of robust and efficient NTF algorithms.

The optimal choice of a free parameter in a specific cost function depends on a statistical distribution of data and additive noise, thus various criteria and algorithms (updating rules) should be applied for estimating the basis matrices $\boldsymbol{A}_k$ and the source matrix $\boldsymbol{S}$, depending on *a priori* knowledge about the statistics of noise or errors. It is worth mentioning that we can use three different strategies to estimate common factors (the source matrix $\boldsymbol{S}$). In the first approach, presented in this paper, we use two different cost functions: a global cost function (using unfolded column-wise matrices: $\bar{\boldsymbol{X}}$, $\bar{\boldsymbol{A}}$ for frontal slices of 3D tensors) to estimate the common factors $\boldsymbol{S}$, i.e., the source matrix $\boldsymbol{S}$; and local cost functions to estimate the slices $\boldsymbol{A}_k$, $(k = 1, 2, ..., K)$. However, instead of using the unfolded matrices for the NTF2 model to estimate $\boldsymbol{S}$, we can use the averaged matrices defined as $\widehat{\boldsymbol{X}} = \sum_k \boldsymbol{X}_k \in \mathbb{R}^{I \times T}$ and $\widehat{\boldsymbol{A}} = \sum_k \boldsymbol{A}_k \in \mathbb{R}^{I \times R}$. Furthermore, it is also possible to apply a different approach by using only a set of local cost functions, e.g., $D_k(\boldsymbol{X}_k || \boldsymbol{A}_k \boldsymbol{S}) = 0.5 || \boldsymbol{X}_k - \boldsymbol{A}_k \boldsymbol{S} ||_F^2$. In such a case, we estimate $\boldsymbol{A}_k$ and $\boldsymbol{S}$ cyclically by applying alternating minimization (similar to row-action projection of the Kaczmarz algorithm). We found that such approaches also work quite well for the NTF2 model. The advantage of the last approach is that all the update learning rules are local (slice by slice) and algorithms are generally faster for large data, (especially, if $K >> 1$).

Obviously, 3D NTF models can be transformed to a 2D non-negative matrix factorization (NMF) problem by unfolding (matricizing) tensors. However, it should be noted that such a 2D model is not exactly equivalent to the NMF2 model, since in practice we often need to impose different additional constraints for each slice. In other words, the NTF2 model should not be considered as equal to a standard 2-way NMF of a single unfolded 2-D matrix. The profiles of the stacked (column-wise unfolded) $\bar{\boldsymbol{A}}$ are often not treated as single profiles and the constraints are usually applied independently to each $\boldsymbol{A}_k$ sub-matrix that form the stacked $\bar{\boldsymbol{A}}$. We have been motivated to develop the proposed NTF algorithms for use in three areas of data analysis (especially, EEG data) and signal/image processing: (i) multi-way blind source separation, (ii) model reduction and selection, and (iii) sparse image coding. The proposed models can be further extended by imposing additional, natural constraints such as smoothness, continuity, closure, unimodality, local rank, selectivity, and/or by taking into account a prior knowledge about specific 3D, or more generally, multi-way data. Obviously, there are many challenging open issues remaining, such as global convergence, optimal choice of parameters and uniqueness of a solution when additional constraints are imposed.

5. REFERENCES

[1] S. Amari, *Differential-Geometrical Methods in Statistics*, Springer Verlag, 1985.

[2] "Workshop on tensor decompositions and applications," CIRM, Marseille, France, 2005.

[3] M. Heiler and C. Schnoerr, "Controlling sparseness in nonnegative tensor factorization," in *ECCV*, 2006.

[4] A. Smilde, R. Bro, and P. Geladi, *Multi-way Analysis: Applications in the Chemical Sciences*, John Wiley and Sons, New York, 2004.

[5] M. Berry, M. Browne, A. Langville, P. Pauca, and R. Plemmons, "Algorithms and applications for approximate nonnegative matrix factorization," *Computational Statistics and Data Analysis*, vol. 2006, submitted.

[6] A. Cichocki, R. Zdunek, and S. Amari, "Csiszar's divergences for non-negative matrix factorization: Family of new algorithms," *LNCS*, vol. 3889, pp. 32–39, 2006.

[7] A. Cichocki, S. Amari, R. Zdunek, R. Kompass, G. Hori, and Z. He, "Extended SMART algorithms for non-negative matrix factorization," *LNAI*, vol. 4029, pp. 548–562, 2006.

[8] A. Cichocki and R. Zdunek, "NTFLAB for Signal Processing," Tech. Rep., Laboratory for Advanced Brain Signal Processing, BSI, RIKEN, Saitama, Japan, 2006.

[9] I. Dhillon and S. Sra, "Generalized nonnegative matrix approximations with Bregman divergences," in *Neural Information Proc. Systems*, Vancouver, Canada, December 2005.

[10] M. Kim and S. Choi, "Monaural music source separation: Nonnegativity, sparseness, and shift-invariance," *LNCS*, vol. 3889, pp. 617–624, 2006.

[11] D. D. Lee and H. S. Seung, "Learning the parts of objects by nonnegative matrix factorization," *Nature*, vol. 401, pp. 788–791, October 1999.

[12] M. Morup, L. K. Hansen, C. S. Herrmann, J. Parnas, and S. M. Arnfred, "Parallel factor analysis as an exploratory tool for wavelet transformed event-related EEG," *NeuroImage*, vol. 29, no. 3, pp. 938–947, 2006.

[13] F. Miwakeichi, E. Martnez-Montes, P. A. Valds-Sosa, N. Nishiyama, H. Mizuhara, and Y. Yamaguchi, "Decomposing EEG data into spacetime-frequency components using Parallel Factor Analysis," *NeuroImage*, vol. 22, no. 3, pp. 1035–1045, 2004.

[14] M. Minami and S. Eguchi, "Robust blind source separation by beta-divergence," *Neural Computation*, vol. 14, pp. 1859–1886, 2002.

[15] M. Merritt and Y. Zhang, "An interior-point gradient method for large-scale totally nonnegative least squares problems," *J. Optimization Theory and Applications*, vol. 126, no. 1, pp. 191–202, 2005.